Methane Hydrate: Killer cause of Earth's greatest mass extinction

Uwe Brand[1*], Nigel Blamey[1], Erika Griesshaber[2], Renato Posenato[3], Lucia Angiolini[4], Karem Azmy[5], Enzo Farabegoli[6], Rosemarie Came[7]

[1]Department of Earth Sciences, Brock University, St. Catharines, Ontario L2S 3A1 Canada

[2]Department of Earth and Environment Sciences, Ludwig Maximilian Universität, Theresienstr. 41, 80333 München, Germany

[3]Dipartimento di Fisica e Scienze della Terra, Università di Ferrara, Polo Scientifico-tecnologico, Via Saragat 1, 44100 Ferrara Italy

[4]Dipartimento di Scienze della Terra, Via Mangiagalli 34, Università di Milano, 20133 Milan Italy

[5]Department of Earth Sciences, Memorial University, St. John's, NL A1B 3X5 Canada

[6]Dipartimento di Scienze della Terra e Geologico – Ambientali, Università di Bologna, Via Zamboni 67, 40126 Bologna, Italy

[7]Department of Earth Sciences, The University of New Hampshire, Durham, New Hampshire 03824 U.S.A.

ABSTRACT

The cause for the end Permian mass extinction, the greatest challenge life on Earth faced in its geologic history, is still hotly debated by scientists. The most significant marker of this event is

the negative $\delta^{13}C$ shift and rebound recorded in marine carbonates with a duration ranging from 2000 to 19,000 years depending on localities and sedimentation rates. Leading cause for the event are Siberian trap volcanism and the emission of greenhouse gases with consequent global warming, but other leading contenders are oceanic anoxia and acidification. Measurements of gases vaulted in calcite of end Permian brachiopods and whole rock document significant differences in normal atmospheric equilibrium concentration (NAEC) of gases between modern and end Permian seawaters. The gas composition of the end Permian brachiopod-inclusions reflects dramatically higher seawater carbon dioxide and methane contents leading up to the biotic event. Initial global warming of 8 to 11°C sourced by isotopically-light carbon dioxide from volcanic emissions triggered the release of isotopically-lighter methane from permafrost and shelf sediment methane hydrates. Consequently, the huge quantities of methane emitted into the atmosphere and the oceans accelerated global warming and marked the negative $\delta^{13}C$ spike observed in marine carbonates documenting the onset of the mass extinction period. The rapidity of the methane hydrate emission lasting from several years to thousands of years was tempered by the equally rapid oxidation of the atmospheric and oceanic methane that gradually reduced its warming potential but not before global warming had reached levels lethal to most life on land and in the oceans. Based on measurements of gases trapped in biogenic and abiogenic calcite, the release of methane (of ~ 3 -14 % of total C stored) from permafrost and shelf sediment methane hydrate is deemed the ultimate source and cause for the dramatic life-changing global warming (GMAT > 34°C) and oceanic (negative carbon isotope excursion) changes observed at the end Permian. Global warming triggered by the massive release of carbon dioxide may be catastrophic, but the release of methane from hydrate may be apocalyptic. The end Permian holds an important lesson for humanity regarding the issue it faces today with greenhouse gas emissions, global warming, and climate change.

1. INTRODUCTION

The end Permian was the greatest natural catastrophe experienced by life on Earth with its impact recorded in terrestrial and marine rock archives. About 90 % of marine species, 70 % of terrestrial vertebrate species, 30 % of insect orders and an indeterminate percentage of terrestrial and marine plants succumbed during this catastrophe (e.g., Erwin, 1994; Brand et al., 2012). This devastating mass extinction on Earth became the foundation for the rise of Mesozoic marine and terrestrial life. Important considerations of the end Permian mass extinction are, 1) the close connection in the demise of the marine and terrestrial fauna and flora (e.g., Schneebeli-Hermann, 2013), 2) the rapidity of the onset of this catastrophe (e.g., Brand et al., 2012) and, 3) the age constraint of the end Permian and the extinction event (e.g., Burgess et al., 2014). Numerous causes have been proposed for the catastrophic end Permian mass extinction, which may have acted alone or in concert, but with many researchers favoring a tangled web of interacting and related causes and effects such as global warming, anoxia and/or acidification (e.g., Wignall and Hallam, 1992; Wignall and Twitchett, 1996; Cao et al., 2009; Clarkson et al., 2015). This global event is increasingly associated with Siberian Trap volcanism and the emission of the greenhouse gas CO_2 leading to global warming (e.g., Svensen et al., 2009; Schneebeli-Hermann et al., 2013), with some suggesting that methane from a variety of sources may have played a supporting role (Berner, 2002; Retallack and Jahren, 2008; Brand et al., 2012), while oceanic anoxia was a minor and/or local player (e.g., Brand et al., 2012; Garbelli et al., 2015), and acidification only played a role during the early Triassic (e.g., Clarkson et al., 2015).

Carbonates may contain gas trapped in minuscule inclusions that are readily released during crushing and subsequently may be analyzed by mass spectrometer for their make-up and

compositions (e.g., Blamey, 2012). If the gases in these inclusions were trapped during formation of the carbonate and remained sealed/vaulted in the inclusions, then they may represent ambient seawater gas conditions and with Henry's Law and mass balance calculations may provide a link between the hydrosphere and atmosphere (Brand et al., 2015). Brachiopods are ideal archives because they precipitate low-in-Mg calcite shells that are quite resistant to post-depositional alteration (Brand and Veizer, 1980; Brand, 2004), and they incorporate carbon and oxygen isotopes into shell calcite in equilibrium with ambient seawater (cf. Lowenstam, 1961; Brand et al., 2013, 2015). Furthermore, to reflect ambient environmental oceanographic conditions, carbonates including brachiopods must incorporate dissolved gases and water into shell calcite gas inclusions from seawater without modification of the normal atmospheric equilibrium parameters (NAEC; Fig. 1). Gas inclusions in modern brachiopods such as *Terebratalia transversa* (Fig. 2a) and *Liothyrella uva* (Fig. 2b) may be quite small but ubiquitous (Fig. 3) and thus satisfy the requirements demanded by the standard operating procedures of the analytical crush fast-scan mass spectrometry (CFS-MS) method for measuring trapped gases in inclusions.

Our objectives are, 1) to characterize the gases in modern brachiopods and coral and use them as references and baselines for evaluating gases measured in end Permian brachiopod shells and whole rock, 2) decipher the atmospheric and oceanographic conditions leading up to the end Permian, and 3) identify the ultimate source/trigger for the catastrophic global warming and climate change event during the biggest mass extinction in Earth history.

2. METHODS

Modern brachiopods were evaluated for evidence of gas inclusions in their calcite fibers and prisms. Extraction and analysis of volatiles was performed by the crush-fast scan (CFS)

97 method (Norman and Blamey, 2001; Blamey, 2012), at room temperature offers low detection
98 limits (>1.2e-15 mol, 2□), with negligible quartz-blank readings (>4.14e-14 mols CH_4 to 1.0e-16
99 mols Ar), analytical gas signals with precision of better than 0.5 % (1□), and gas content of
100 Standard NB-84 is within 1 % of reported contents (Blamey et al., 2015). Each gas burst was
101 analyzed for H_2, He, CH_4, N_2, O_2, Ar, and CO_2, using two Pfeiffer Prisma "residual-gas" quadrupole
102 mass spectrometers operating in fast-scan, peak-hopping mode at room temperature. A total of
103 37 gas measurements were made on seven modern biogenic samples, and a total of 52 gas
104 measurements on seven end Permian brachiopod and whole rock samples. A total of 89
105 normalized gas measurements (weighted by gas burst size) reported in mol % are listed in the
106 Appendix. Due to the new nature of the gas inclusion method, a detailed description is provided
107 in the Supplementary section.

108 **3. Gas Classification and Screening**

109 The question arises as to whether brachiopod shells contain sufficient quantities of gas
110 for measurement by mass spectrometer? Excessive electron energy applied to a polished
111 surface of a brachiopod shell caused bubbles to form below the platinum coating (Fig. 3). The
112 bubbles of gas and/or fluid may be derived from degradation of organic tissue sourced from
113 between and within the fibers, or from constituents trapped during formation of the biogenic
114 fibers. Large and small pores are present in the shells of *Terebratalia transversa* and *Liothyrella*
115 *uva*, but only ones that are vaulted may be suitable for gas analysis (Fig. 2). The physical
116 evidence supports the presence of suitable pores but that is only the first step in the evaluation
117 process. Further, we must establish that the gas contents of brachiopod and other marine
118 archives reflect NAEC of gases in seawater and consequently of the atmosphere. A plot of gas
119 contents of several modern brachiopods and one coral shows that they indeed reflect

equilibrium seawater and atmospheric compositions, which confirms their reliability as archives of trapping environmental gases for atmospheric gas reconstruction (Fig. 1).

Further screening must be conducted to test for their reliability in retaining NAEC of gases with the passage of time. Gas results of modern brachiopods plot in an area characterizing marine conditions in equilibrium with the atmosphere defined by CO_2/CH_4 ratios ranging from 10 to 1000, and by N_2/Ar ratios ranging from 35 to 130 (Table 1), on the modified classification scheme originally proposed by Norman et al. (1994; Norman and Moore, 1999; Moore et al., 2001; Fig. 4, Field 1). Field boundaries have been constructed to accommodate ranges of gas measured in fresh-water carbonates (Field 2), as well as brachiopods that have experienced post-depositional alteration (Field 3) and gas concentration variation in marine carbonates with changes in atmospheric chemistry (Field 4) and changes in chemistry with or without bacterial carbonate reduction (Field 5). In contrast to the modern biogenic carbonates (Field 1), the end Permian brachiopods and carbonates from northern Italy plot into field 4 designated modified Marine [change in chemistry] characterized by secular changes in seawater/atmospheric chemistry (Fig. 4). By virtue of their excellent preservation (Brand et al., 2012), and constrained by their values within field 4, the gas obtained from the end Permian samples should reflect ambient seawater/atmospheric conditions during time of formation.

4. Carbon Isotope Excursion (CIE)

The negative carbon isotope excursion (nCIE) in marine carbonates has been long recognized as an important marker of the end Permian (PT) event at Meishan and other localities, and it may vary by as much as 6.5 ‰ (Fig. 5; e.g., Jin et al., 2000; Retallack and Krull, 2006; Garbelli et al., 2015). However, its origin, source and duration remain problematic (Berner, 2002), and consequently, a definitive cause and mechanism for the nCIE and PT event

still elude us. A recent study by Burgess et al. (2014) provided an updated set of more precise ages, and thus improved times for the onset, duration and offset of the mass extinction event that are essential in better understanding the reorganization of the carbon cycle and identifying a potential source for the trigger and kill mechanisms. Burgess et al. (2014) suggested, depending on sedimentation rate, the negative CIE shift and its rebound lasted between 2.1 to 18.8 thousand years, while slightly pre-dating the onset of the maximum extinction (cf. Brand et al., 2012).

4.1 Meishan – northern Italy nCIE Trends

In conjunction with results from Meishan, precisely placed and well-preserved samples from the end Permian succession in northern Italy provide the requisite high-resolution database (Brand et al., 2012) to shed light on the cause of the greatest mass extinction. Gas ratios of the end Permian samples fall into Field 4 (marine carbonates with changing chemistry, Fig. 4), and with methane dominating the greenhouse gas content relative to that of modern counterparts (Tables 1, 2). A closer examination of the time interval preceding the mass extinction clearly shows a negative CIE of about 3.5 ‰ leading up to the major event at Meishan and in part in northern Italy (Fig. 6A), while a smaller but distinct negative $\delta^{13}C$ excursion in the lower half of bed 24e at Meishan is also recognized in the results from Italy (Fig. 6B; cf. Brand et al., 2012). These two negative carbon isotope excursions are designated 'Pulse 1' and 'Pulse 2', which also correspond to negative excursions of the brachiopod $\delta^{18}O$ values from Italy (Fig. 6C, expressed in T°C). Based on the $\delta^{18}O$ values of conodonts, water temperatures at Meishan remained around 25°C and reached higher ones only during deposition of Bed 26 and subsequent ones (Joachimski et al., 2012), whereas those from northern Italy based on shallow water brachiopods ranged from 30° up to 35°C just before the extinction (Fig. 6C; Brand et al.,

166 2012). The water temperatures associated with Pulse 2 are sufficiently high (Table 3) to cause
167 stress for many tropical and polar organisms because of their poor acclimation capacity (e.g.,
168 Stillman, 2003; Peck et al., 2010), leading to widespread lethal environmental conditions and
169 possibly mass die-off.

170 The measured CO_2/CH_4 ratios of the end Permian samples are relatively low (Table 2)
171 and initially invariant but marked by two distinct pulses corresponding to the nCI and nOI
172 excursions and warming trend pulses noted at Meishan and northern Italy (Fig. 6D). The first gas
173 pulse corresponds to the small but significant nCIE noted in the lower half of Bed 24e at
174 Meishan and to corresponding levels in northern Italy (Fig. 6A, B). The subsequent rise in the gas
175 ratio may be related to the rapid oxidation of some of the released methane to carbon dioxide
176 (Berner, 2002). The second pulse and more pronounced fall in the CO_2/CH_4 ratio document a
177 significant upswing in methane emission just before the onset of the end Permian biotic crisis,
178 and it corresponds well with the world-wide observed nCIE and water temperature changes
179 observed in northern Italy and Tibet (cf. Garbelli et al., 2015).

180 **5. End Permian Atmospheric Conditions**

181 Generally, uncertainties of timing and duration of events limit the interpretations of
182 many important biologic/geologic events among them the end Permian mass extinction (e.g.,
183 Rampino et al., 2000; Posenato, 2009; Shen et al., 2010). But this critical issue of time has been
184 since resolved with results from recent publications that allows for the improved geochemical
185 characterization of the source(s) for this most dramatic of events (Brand et al., 2012; Burgess et
186 al., 2014). The issue of ambient gas content and concentration are resolved by the crush fast-
187 scan method that measures gas trapped in tiny pores of select modern and fossil materials
188 reflecting marine and atmospheric systems (Tables 1, 2; cf. Brand et al., 2015). The screening

chart easily distinguishes preserved material from altered ones (cf. altered Selong material from China, Field 3, Fig. 4; Table 2). Consequently, only the best material with preserved NAEC of gases in seawater will be used in characterizing the end Permian atmosphere (Field 4, Fig. 4).

The greenhouse gas build-up prior to the event was driven mostly by the emission of carbon dioxide from Siberian Trap volcanic deposits (e.g., Svensen et al., 2009), whereas methane emissions from hydrates/clathrates are a leading contender for 'pushing' the global warming process over the sustainable limit (e.g., Krull and Retallack, 2000; Retallack and Jahren, 2008). Armed with pre-industrial atmospheric conditions, we note a gradual but rising shift in both CO_2 and CH_4 by the 1980's (Table 3). These time periods clearly define the relationship between atmospheric and marine hydrospheric conditions and those of the ambient biogenic marine carbonates (Fig. 1).

5.1 Model and Measured Parameters

A number of researchers modeled gas ratios for the end Permian (e.g., Berner, 2002; Kiehl and Shields, 2005; Retallack and Jahren, 2008; Brand et al., 2012) ranging from 1700 ppm to 3,550 ppmv for CO_2, and 'constant' 0.7 ppmv for CH_4 (end Perm (a), end Perm (d1), Table 3). A supplemental parameter of fixed CO_2 and variable CH_4 is added to the discussion and this segment (end Perm (c), Table 3). There are potentially a number of concerns with these modeled atmospheric parameters, such as, 1) the global mean atmospheric temperatures derived from these parameters may not be high enough to bring about a biotic crisis, and 2) there was insufficient negative carbon to produce the world-wide observed nCIE at the end Permian (e.g., Berner, 2002).

The first two model cases assume no change or contribution by methane to the global climate change scenario (end Perm (a) and (b), Table 3), and with $Brach_{ratios}$ (780 and 476) well

212 above those measured in modern and end Permian counterparts. Clearly, the two modeled
213 parameters are outside the realm of possibility of gas ratios measured in end Permian
214 brachiopods (Table 2). It is apparent that the flaw does not rest with the postulated CO_2
215 contents but with the methane component, and consequently alternatives to the constant and
216 static CH_4 composition must be contemplated.

217 The third model conditions suggested (end Perm (c), Table 3) is equally unsatisfactory
218 with proposed modern carbon dioxide levels but increased methane component, since the
219 global GMAT is quite insufficient to trigger a biotic crisis. Furthermore, pH levels with these
220 atmospheric parameters are unlikely to have caused any concerns with oceanic acidification,
221 unlike the ones calculated for the first two model conditions (Table 3).

222 It has been proposed that CO_2 may have varied for the end Permian between 1700 and
223 3550 ppm (Table 3). With the atmospheric ratio of 27.8 based on the average brach ratio of 4.3
224 determined for the end Permian, we are able to determine the methane concentration during
225 the end Permian. In this instance, CH_4 may have varied between a low of 61 and a high of 126
226 ppmv with corresponding amounts of carbon dioxide (Table 3). Global temperatures and
227 seawater pH levels are sufficiently high and low, respectively, and with these gas parameters
228 environmental conditions would be a challenge for terrestrial and marine life.

229 5.2 End Permian atmosphere

230 A detailed evaluation of the gas components and their trends suggests that during pre-
231 Pulse time the brach ratio was about 4.3, but during Pulse 1 it dropped to 3.3, and then to 2.2
232 during Pulse 2 with recoveries in between (Fig. 6D, Table 3). Maintaining the appropriate ratios
233 and modeled atmospheric concentrations of carbon dioxide, the methane content of the
234 atmosphere may have varied from a low of 61 ppmv during pre-Pulse time to 121 ppmv during

235 Pulse 1 and increased to possibly even 245 ppmv at the onset of the biotic crisis (Fig. 6D, Table
236 3). Considering the global warming potential of both CO_2 and CH_4, the Global Mean Air
237 Temperature (GMAT) may have varied from 29 to 34°C, which correspond well within several
238 degrees to water temperatures recorded by tropical end Permian brachiopods from northern
239 Italy (Brand et al., 2012) and Tibet (Garbelli et al., 2015). The slight offset may be related to
240 differences between SST and habitat temperatures of shallow water brachiopods. Overall the
241 temperature impact by methane would be significant but of short duration because of its fast
242 oxidation to carbon dioxide (Berner, 2002) as evidenced by the reversal in CO_2/CH_4 ratio just
243 before Pulse 2 (Fig. 6D). In addition, the determined pH values of 7.85 to 7.69 are sufficiently
244 low to suggest some acidification of seawater during this critical time period.

245 **6.0 Methane Source**

246 The question arises, is the emission of gas from Siberian Trap volcanism sufficient to
247 cause both the exacerbated warming and negative carbon isotope shift experienced during the
248 end Permian (Fig. 7a)? The answer on both accounts is in the negative (e.g., Berner, 2002;
249 Retallack and Jahren, 2008; Brand et al., 2012), and thus a new question must be posed whether
250 there is sufficient methane stored in permafrost and marine sediments upon release to cause a
251 major perturbation of the global carbon cycle with subsequent warming and its accompanying
252 nCIE (Fig. 7b). If the amount of methane in the atmosphere varied from 61 to about 245 ppmv
253 based on gas measured in end Permian marine carbonates (Table 3), we should be able to
254 determine the amount of stored isotopically-light methane that would need to be released from
255 these two reservoirs. With about 2,800 Gt of C stored in the two major sinks of marine
256 sediments and permafrost today (Kvenvolden, 1998; Boswell and Collett, 2011), and under
257 present climatic conditions there is a miniscule release of 0.1 % methane hydrates over the last

100 years from marine sediments amounting to an atmospheric contribution of 1125 ppmv CH_4 (Table 4; Ruppel, 2011). We performed simple mass balance calculations of methane release for a period of 100 years and distributed these evenly among the permafrost and marine sediment reservoirs. During the pre-Pulse stage atmospheric methane attained a level of about 61,000 ppbv (Table 3) and when combined with the emission rate of 1125ppbv/100 years equal to 0.1 % from methane hydrate gives a contribution of 2.7 % and 4.9 % from the marine sediment and permafrost reservoirs, respectively, for a total value of about 98 Gt C/100 years (Table 4). For Pulse 1, the amount of methane released would have been equivalent to 5.4 and 9.7 %, respectively, for a total contribution of 194 Gt C/100 years (Table 4). For Pulse 2, the amount of methane released would have been equivalent to 10.9 and 19.6 %, respectively, for a total contribution of about 392 Gt C/100 years (Table 4). These contributions equate to a yearly rate ranging from 1 .0 to 3.9 Gt C (CH_4), which are similar to emission rates of 0.8 to 2.1 Gt C/y calculated for C-isotope depleted carbon (Svensen et al., 2009) derived from the experimental metamorphism of carbon rich sediments. This process would be coeval to the release of gas by the Siberian Traps and not be limited to just the 'end' of the Permian just slightly preceding the biotic event and, furthermore, is not supported by the rapid onset of the well-documented nCIE (Figs. 5, 6).

It is clear from this discussion that after extensive warming of the Earth caused by carbon dioxide emission from Siberian Trap volcanics (Fig. 7a), eventually the major and sudden release of methane from hydrate during the end Permian, global temperatures reached levels detrimental to marine and terrestrial life, and its oxidized product (highly negative carbon dioxide) caused the prominent nCIE documented in many global marine and terrestrial sequences (cf. Berner, 2002; Schneebeli-Hermann et al., 2013). Thus, the measured gas content of marine carbonates from the end Permian support the concept that methane derived from

282 permafrost and marine sediments was ultimately the major driving force and cause for the
283 greatest biotic crisis (Fig. 6). In contrast, the survivors of this event probably resided in deeper
284 waters and were not affected by the warming oceans until much later after the main event (Fig.
285 5).

286 **CONCLUSIONS**

287 Biogenic and abiogenic carbonates from the end Permian succession in northern Italy carry gas
288 in inclusions that formed in NAEC with those of the ambient seawater and atmosphere. Gas
289 measured in inclusions suggests two pulses of methane emission before the end Permian mass
290 extinction event.

291 Carbon dioxide derived from Siberian Trap volcanism with its $\delta^{13}C$ value of about -6 ‰ would
292 bring about a warming of about 6°C and a shift in marine carbonate $\delta^{13}C$ values by about -2‰.
293 The rapid addition of isotopically lighter methane (~ -60 ‰) to the global atmosphere and
294 hydrosphere would bump up the average global temperature to above 29°C and, after
295 oxidation, the $\delta^{13}C$ signature in marine carbonates to the commonly recorded carbon isotope
296 composition ranging from -2 to -7 ‰.

297 The emission of carbon dioxide from volcanic deposits may have started the world onto the road
298 of mass extinction, but it was the release of methane from shelf and permafrost hydrates that
299 was the ultimate cause for the catastrophic event at the end Permian.

300 Our observations on the global warming process, such as the release of massive amounts of
301 carbon dioxide and subsequently followed by methane, and their impacts on life during the end
302 Permian has important lessons for humanity and the problems associated with climate change
303 in the 21st century.

Acknowledgements

We thank NSERC, NSF, Brock, Memorial, New Hampshire, Ferrara, Milano & Bologna Universities for financial support.

References

Berner, R. A. (2002). "Examination of hypotheses for the Permo-Triassic boundary extinction by carbon cycle modeling." Proceedings National Academy of Sciences **99**: 4172-4177.

Blamey, N. J. F. (2012). "Composition and evolution of crustal, geothermal and hydrothermal fluids interpreted using quantitative fluid inclusion gas analysis." Journal of Geochemical Exploration **116-117**: 17-27.

Blamey, N. J. F., et al. (2012). “Understanding detection limits in fluid inclusion analysis using an incremental crush fast scan method for Planetary Science”. 43rd Lunar and Planetary Science 1035.

Blamey, N. J. F., et al. (2015). "Evidence for methane in martian meteorites" Nature Communications **6**:7399: 1-7.

Boswell, R. and T. S. Collett (2011). "Current perspectives on gas hydrate resources." Energy & Environmental Science **4**: 1206-1211.

Brand, U. (2004). "Carbon, oxygen and strontium isotopes in Paleozoic carbonate components: an evaluation of original seawater-chemistry proxies." Chemical Geology **204**: 23-44.

Brand, U. and J. Veizer (1980). "Chemical diagenesis of a multicomponent carbonate system: 1, Trace elements." Journal of Sedimentary Petrology **50**: 1219-1236.

Brand, U., et al. (2012). "The end-Permian mass extinction: a rapid volcanic CO2 and CH4 -climatic catastrophe." Chemical Geology **322-323**: 121-144.

Brand, U., et al. (2013). "Oxygen isotopes and MgCO3 in brachiopod calcite and a new paleotemperature equation." Chemical Geology **359**: 23-31.

Brand, U., et al. (2015). "Carbon isotope composition in modern brachiopod calcite: a case of equilibrium with seawater?" Chemical Geology **411**: 81-96.

Brand, U., et al. (2015). “Methane Clathrate: Killer cause of Earth’s greatest mass extinction”. GSA Abstracts.

Burgess, S. D., et al. (2014). "High-precision timeline for Earth's most severe extinction." Proceedings

National Academy of Science **111**: 3316-3321.

Cao, C., et al. (2009). "Biogeochemical evidence for euxinic oceans and ecological disturbance presaging the end-Permian mass extinction event." Earth and Planetary Science Letters **281**: 188-201.

Clarkson, M. O., et al. (2015). "Ocean acidification and the Permo-Triassic mass extinction." Science **348**: 229-232.

Erwin, D. H. (1994). "The Permo-Triassic extinction." Nature **367**: 231-236.

Garbelli, C., et al. (2015). "Neotethys seawater chemistry and temperature at the dawn of the end Permian mass extinction." Gondwana Research.

Jin, Y. G., et al. (2000). "Pattern of marine mass extinction near the Permian-Triassic boundary in South China." Science **289**: 432-436.

Joachimski, M. M., et al. (2012). "Climate warming in the latest Permian and the Permian-Triassic mass extinction." Geology **40**: 195-198.

Kiehl, J. T. and C. A. Shields (2005). "Climate simulation of the latest Permian: implications for mass extinction." Geology **33**: 757-760.

Kvenvolden, K. A. (1998). “A primer on the occurrence of gas hydrates”. In Henriet, J.P. and Mienert, J. (eds) “Gas hydrates: relevance to world margin stability and climate change”. Geological Society, London Special Publications **137**, 9-30.

Lowenstam, H. (1961). "Mineralogy, O^{18}/O^{16} ratios, and strontium and magnesium contents of recent and fossil brachiopods and their bearing on the history of the oceans." Journal of Geology **69**: 241-260.

Moore, J. N., Norman, D. I., and B. M. Kennedy (2001). “Fluid inclusion gas compositions from an active magmatic hydrothermal system: a case of The Geysers geothermal field, USA”. Chemical Geology **173**: 3–30.

Norman, D. I. and N. J. F. Blamey (2001). “Quantitative analysis of fluid inclusion volatiles by a two quadrupole mass spectrometer system”. ECROFI XVI, 341–344.

Norman, D. I. and J. N. Moore (1999). “Methane and excess N_2 and Ar in geothermal fluid inclusions”. Proceedings: Twenty-fourth Workshop of Geothermal Reservoir Engineering, Stanford University, Stanford, California, January 22-24, 1999, 233-240.

Norman, D.I. and J. A. Musgrave (1994). “N_2–Ar–He compositions in fluids inclusions: indicators of fluid source”. Geochimica et Cosmochimica Acta **58**: 1119–1131.

Peck, L. S., et al. (2010). "Poor acclimation capacities in Antarctic marine ectotherms." Marine Biology **157**: 2051-2059.

Posenato, R. (2009). "Survival patterns of macrobenthic marine assemblages during the end-Permian

mass extinction in the western Tethys (Dolomites, Italy)." Palaeogeography, Palaeoclimatology, Palaeoecology **280**: 150-167.

Rampino, M. R., et al. (2000). "Tempo of the end-Permian event: high resolution cyclostratigraphy at the Permian-Triassic boundary." Geology **28**: 643-646.

Retallack, G. J. and A. H. Jahren (2008). "Methane release from igneous intrusions of coal during the Late Permian extinction events." Journal of Geology **116**: 1-20.

Retallack, G. J. and E. S. Krull (2006). "Carbon isotopic evidence for terminal-Permian methane outbursts and their role in extinctions of animals, plants, coral reefs, and peat swamps." Geological Society of America, Special Paper **399**: 249-268.

Ruppel, C. D. (2011). "Methane hydrates and contemporary climate change." Nature Education Knowledge **3**: 29-38.

Schneebeli-Hermann, E., et al. (2013). "Evidence for atmospheric carbon injection during the end-Permian extinction." Geology **41**: 579-582.

Shen, S. Z., et al. (2010). "End-Permian mass extinction and paleoenvironmental changes in Neotethys: evidence from an oceanic carbonate section in southwestern Tibet." Global and Planetary Change **73**: 3-14.

Stillman, J. H. (2003). "Acclimation capacity underlies susceptibility to climate change." Science **301**: 65.

Svensen, H., et al. (2009). "Siberian gas venting and the end-Permian environmental crisis." Earth and Planetary Science Letters **277**: 490-500.

Wignall, P. B. and A. Hallam (1992). "Anoxia as a cause of the Permian/Triassic extinction: facies evidence from northern Italy and the western United States." Palaeogeography, Palaeoclimatology, Palaeoecology **93**: 21-46.

Wignall, P. B. and R. J. Twitchett (1996). "Oceanic Anoxia and the End Permian Mass Extinction." Science **272**: 1155-1158.

Yin, H., et al. (2001). "The global stratotype section and point (GSSP) of the Permian-Triassic boundary." Episodes **24**: 102-114.

Fig. 1. _13C excursion, faunal disappearances and gas compositions about the end Permian (GSSP section at Meishan, China). Atmospheric greenhouse gas wasdominated by CO2prior to the event with a sudden surge in CH4during the latest stage leading into the event. Stratigraphy of Meishan section is from Yin et al.(2001), whereas faunal decline and carbon isotope trend are from Jin et al. (2000), and duration of the mass extinction period is from Burgess et al. (2014).

Fig. 2. Normal atmospheric equilibrium contents of gases in seawater and associated modern biogenic carbonates. The NAEC line represents equilibrium contents(dissolved) of carbon dioxide in modern seawater at temperatures ranging from 0 to 40◦C (Weiss, 1974). The SI, FH and I

(black diamonds) are CO2contents ofmodern biogenic carbonates (brachiopods and coral) from Signy Island, Friday Harbor and Indonesia of shallow water depth (<100 m; Table 1).

Fig. 3. Scanning electron micrographs of secondary and tertiary layers in the end Permian brachiopod Comelicania sp. indet. from northern Italy. (A) Close-up ofwell-preserved secondary layer fibers showing the typical keel and saddle outlines and micro pores (structural defects) that may contain dissolved gases and seawatertrapped during precipitation of the carbonate. (B) Close-up of well-preserved tertiary layer stacked columns with growth brands (cf. Goetz et al., 2009) and micropores (structural defects) formed during the low-Mg calcite formation process.

Fig. 4. High-resolution field-emission scanning electron micrographs of micro- and nano-structures within components of layers of modern brachiopods. (A) Close-up of gaps between fibers of the secondary layer in Notosaria nigricans created after hydrothermal removal of organic tissue. (B) Close-up and distribution ofnanopores (arrows point to some pores) created by the hydrothermal removal of organic tissue in secondary layer fibers of Notosaria nigricans. Supplementary Figs.1, 2 provide locality context.

Fig. 5. Diagenetic screening of the brachiopod and whole rock material fromthe end Permian Bellerophon and Werfen Formations, northern Italy. Sr/Mn and _13C values are used to discriminate between altered and preserved carbonates(cf. Brand and Veizer, 1980). Samples in solid colors were chosen for gas analysis based on preservation status (geochemical and microstructural evidence).

Fig. 6. Gas ratios of CO2, CH4, N2and Ar captured in vaulted pores of modern (C – Huinay, Chile; FH – Friday Harbor, USA; SI – Signy Island, Antarctica)and end Permian brachiopods and limestone of northeastern Italy (Table 2). Classification consists of five fields: Field 1 – Marine Carbonates: carbonates in gasequilibrium with seawater and atmosphere; Field 2 – Meteoric Carbonate: carbonates in gas equilibrium with freshwater system; Field 3 – Diagenesis: diageneticallyaltered material; Field 4 – modified Marine Carbonates: carbonates with gas ratios shifted due to changes in seawater chemistry; and Field 5 – modified MarineCarbonates: carbonates with gas ratios shifted due the change in seawater chemistry and bacterial carbonate reduction. Atmospheric CO2/CH4– N2/Ar ratio includedfor reference; general gas classification scheme and magmatic field are modified after Norman and Musgrave (1994).

Fig. 7. Details of _13C values, seawater temperatures, and gas content excursions at Meishan, China and northeastern Italy. Shaded field represents mass extinctionperiod during the end Permian. Information: stratigraphy (Yin et al., 2001); column A: carbon isotope trends (China – Jin et al., 2000); column B: carbon isotope trend(northern Italy – Brand et al., 2012); column C: seawater temperatures (China – Joachimski et al., 2012; northern Italy – Brand et al., 2012); column D: changingCO2/CH4gas ratios of this study. Pulses 1 and 2 correlate with trend in _13C values from China and northern Italy, seawater temperatures and measured CO2/CH4gas ratios. Gas symbols as in Fig. 6.

Fig. 8. Sequence of events before and during the end Permian mass extinction. Panel (a) represents extensive Siberian Trap Flood volcanism and emission of the greenhouse gas CO2 leading to climatic warming, and panel (b) documents the subsequent release of massive amounts of methane (CH4) hydrate from permafrost and marine shelf sediments and increased global warming (cf. Tables 3, 4). The contribution of methane from either permafrost and/or

marine sediments is open for debate. Note: GMAT – Global Mean Annual Temperature; SL – sea level.

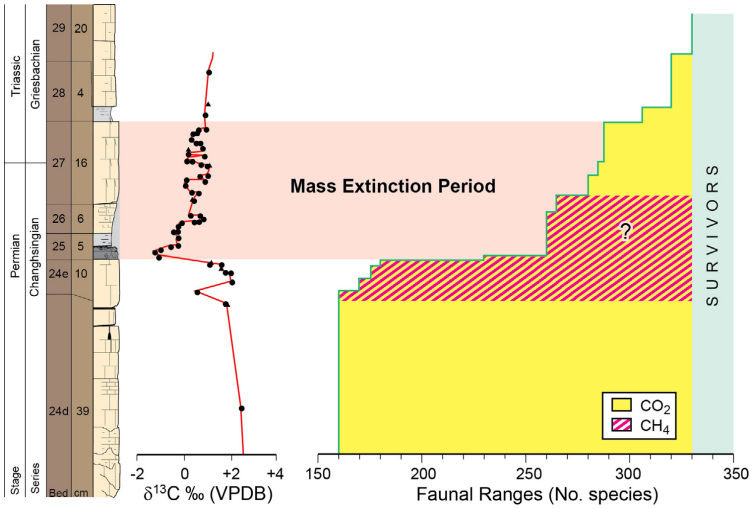

Figure 1

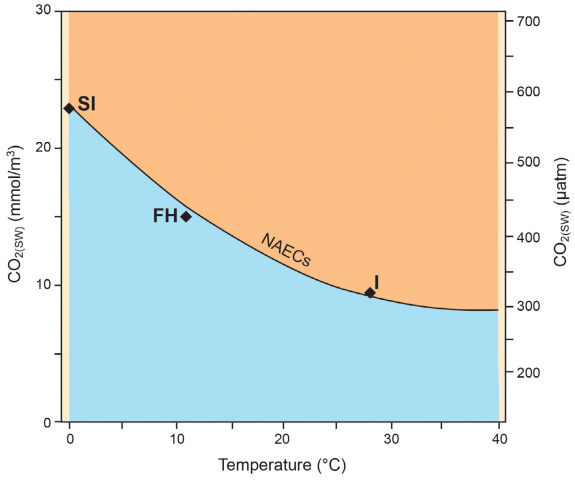

Figure 2

493 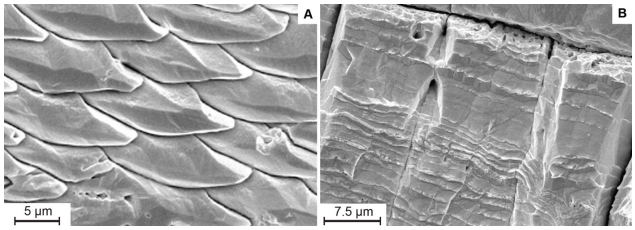

494 Figure 3

495

496 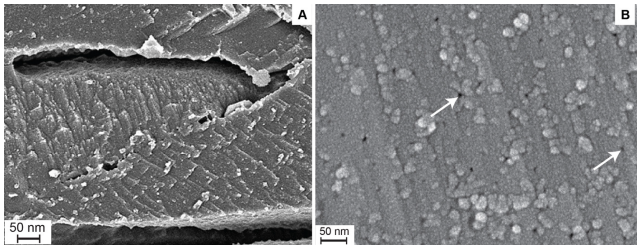

497 Figure 4

498 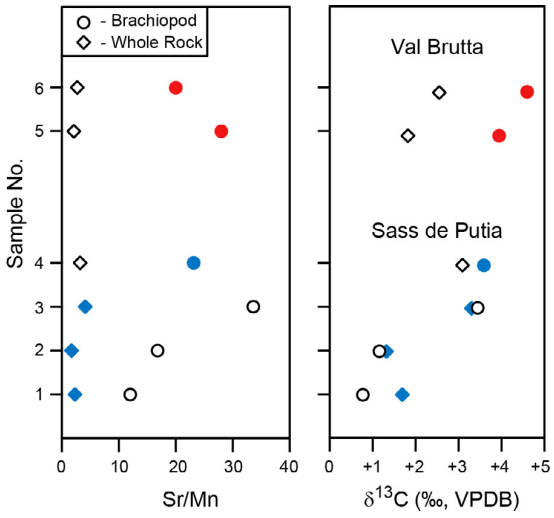

499 Fig. 5

500

501

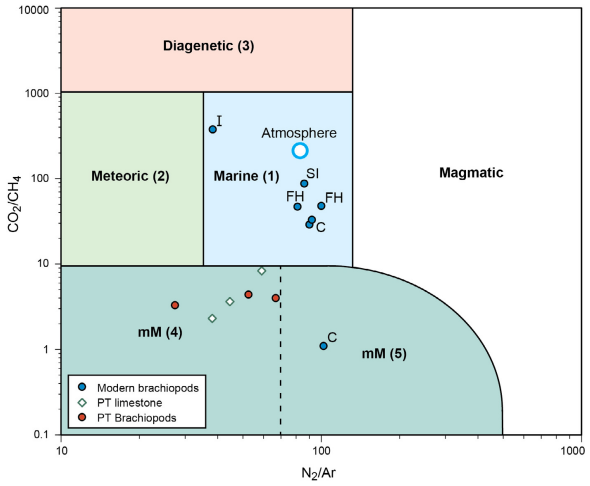

502

503 Fig. 6

504

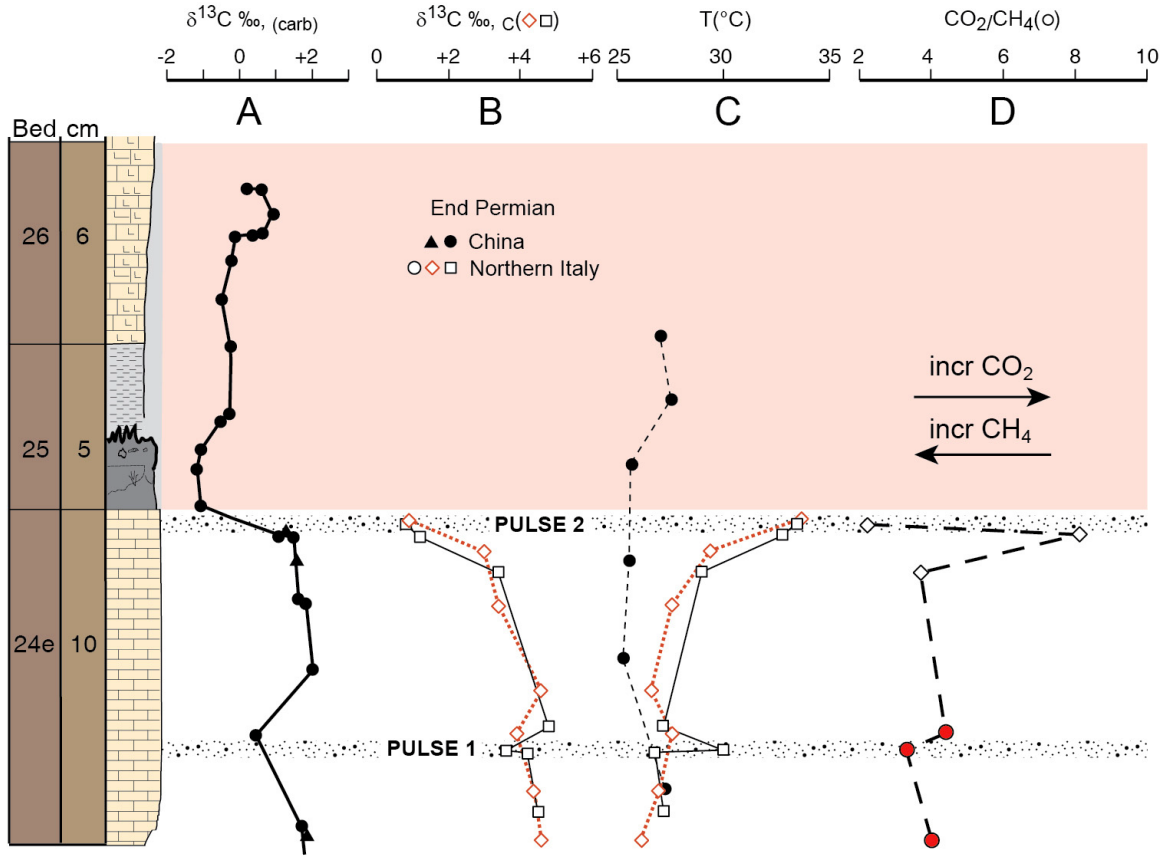

505

506 Fig. 7

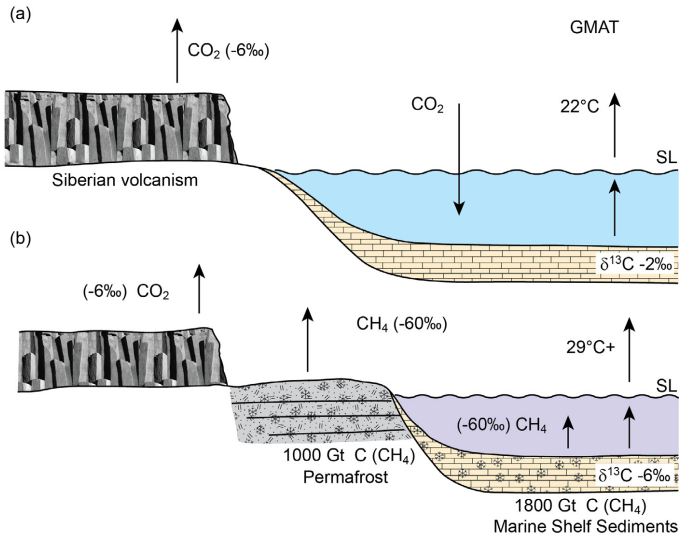

507

508

509 Fig. 8

510

511